Integration of Clinical Data Collected at Different Times for Virtual Surgery in Single Ventricle Patients: A Case Study

Chiara Corsini,[1] Catriona Baker,[2] Alessia Baretta,[1] Giovanni Biglino,[2] Anthony M. Hlavacek,[3] Tain-Yen Hsia,[2] Ethan Kung,[4,5] Alison Marsden,[5] Francesco Migliavacca,[1] Irene Vignon-Clementel,[6,7] Giancarlo Pennati,[1] and The Modeling of Congenital Hearts Alliance (MOCHA) Investigators

[1]Laboratory of Biological Structure Mechanics, Department of Chemistry, Materials and Chemical Engineering 'Giulio Natta', Politecnico di Milano, Milan, Italy; [2]Centre for Cardiovascular Imaging, UCL Institute of Cardiovascular Science, and Great Ormond Street Hospital for Children, NHS Foundation Trust, London, UK; [3]Division of Pediatric Cardiology, Department of Pediatrics, Medical University of South Carolina, Charleston, SC, USA; [4]Mechanical Engineering Department, Clemson University, Clemson, SC, USA; [5]Mechanical and Aerospace Engineering Department, University of California San Diego, San Diego, CA, USA; [6]INRIA Paris-Rocquencourt, Le Chesnay Cedex, France; and [7]Laboratoire Jacques-Louis Lions, UPMC Université Paris 6, Paris, France

(*Received 12 May 2014; accepted 5 September 2014; published online 25 October 2014*)

INTRODUCTION

Pre-operative planning through mathematical modeling has been continuously developing as a powerful approach for clinical decision making in complex congenital heart diseases (CHD), such as

ABBREVIATIONS

APC	Aorto-pulmonary collateral vessels
BDG	Bi-directional Glenn
BSA	Body surface area
CO	Cardiac output
CHD	Congenital heart disease
IVC	Inferior vena cava
LB	Lower body
LPM	Lumped parameter model
MRI	Magnetic resonance imaging
O_2	Oxygen
PA	Pulmonary artery
PVR	Pulmonary vascular resistance
PVWP	Pulmonary venous wedge pressure
RPA	Right pulmonary artery
SVC	Superior vena cava
SVR_{LB}	Lower body systemic vascular resistance
SVR_{UB}	Upper body systemic vascular resistance
3D	Three-dimensional
UB	Upper body
VVC	Veno-venous collateral vessel

Address correspondence to Giancarlo Pennati, Laboratory of Biological Structure Mechanics, Department of Chemistry, Materials and Chemical Engineering 'Giulio Natta', Politecnico di Milano, Milan, Italy. Electronic mail: giancarlo.pennati@polimi.it

single ventricle defects,[4,5,8,15,22] and has been proving itself as the future of personalized medicine. In order to build a reliable patient-specific pre-operative model, it is mandatory to collect as much clinical data as possible. Patients with single ventricle physiology are usually palliated with a multi-staged procedure consisting of three operations performed in the first few days, months and years of life, respectively, gradually re-directing pulmonary flow to bypass the underdeveloped ventricle.[6] Detailed hemodynamic data, however, are routinely collected only prior to each palliative stage. While the first surgical stage can involve multiple surgical alterations, it generally involves a shunt placement between a systemic artery, e.g., the aorta or the innominate artery, and a main pulmonary artery (PA) branch. Stage 2 consists of shunt removal and connection of the superior vena cava (SVC) to the right pulmonary artery (RPA), either through an end-to-side anastomosis (i.e., bi-directional Glenn-BDG-procedure), or through the original SVC-atrial connection and a patch redirecting the SVC flow to the PAs (i.e., hemi-Fontan procedure), to ensure pulmonary perfusion. The third stage, called the Fontan procedure, is performed by connecting also the inferior vena cava (IVC) to the RPA, thus completing the conversion to a full series circulation.

When cardiovascular complications, such as collateral vessel formation, surgical site stenosis, or heart valve dysfunction, occur as secondary to the CHD, a further treatment is often required while assuring the lowest risk to the patient. For instance, patients with collateral vessel formation might undergo occlusion in the catheterization laboratory. Some patients with surgical site stenosis might undergo balloon dilation and/or stent placement in the catheterization laboratory, while others will require surgical revision. Heart valve dysfunction might be successfully treated with medications that alter cardiac afterload or preload, but some patients might require surgical valve repair or replacement. In these scenarios, mathematical modeling could be useful to predict the hemodynamics following the treatment.

In this study, a stage 2 patient was diagnosed with a major veno-venous collateral vessel (VVC) 4 months after undergoing a BDG procedure. Cardiac catheterization was performed to measure pressures and oxygen (O_2) saturations, and to evaluate the need for a treatment, e.g., VVC device closure. Closure of VVC is often performed in single ventricle patients with stage 2 physiology in order to improve O_2 saturation. However, since closure of these collaterals can have unintended consequences such as an elevation of pulmonary artery pressure or an alteration in systemic blood flow, it would be useful to be able to quantify these changes before exposing the patient to the procedure.

The aim of this study is threefold: (i) to show how to build a patient-specific pre-operative model that describes the hemodynamic scenario preceding VVC occlusion, using the pressure and oxygenation data acquired at the time of VVC treatment, in combination with a more extensive data set (i.e., magnetic resonance imaging-MRI-flows and anatomy along with the usual catheterization pressures and O_2 saturations) collected prior to BDG procedure; (ii) to perform virtual VVC occlusion on the model for quantitative hemodynamics prediction (i.e., pressures, flows and O_2 saturations); and (iii) to verify predicted hemodynamics through comparison with post-operative clinical data.

MATERIALS AND METHODS

Clinical Case

A 4-month-old male patient (body surface area, BSA = 0.30 m^2) with hypoplastic left heart syndrome, initially palliated with a Norwood procedure at stage 1, underwent BDG surgery with left PA stenosis correction. Pre-operatively, cardiac catheterization and MRI examinations were performed, thus collecting pressure, flow and anatomical data.

At 4 months following BDG, the 8-month-old baby was experiencing progressive cyanosis. Therefore, he was scheduled for cardiac catheterization through the existing atrial septal opening, and simultaneous angiocardiography which revealed a large decompressing VVC connecting the distal innominate vein to the lower body (LB), and a smaller secondary collateral originating from the SVC. Furthermore, minor aorto-pulmonary collateral vessels (APC) were detected from the thoracic aorta and right subclavian artery to the distal pulmonary arterial beds. Pressures and O_2 saturations measured during catheterization are reported in Table 1. Other measured values were the heart rate (107 bpm) and the blood hemoglobin content (15.9 g dL^{-1}).

With the aim of improving the low arterial O_2 saturation (61%) of the cyanotic patient, the VVC was occluded with vascular plugs during the catheterization procedure. After occlusion, the BDG pressure increased by 2 mmHg, with a trans-pulmonary gradient of 9 mmHg. Hence, the patient required drug therapy for pulmonary hypertension.

The patient was recruited at the Medical University of South Carolina, Charleston, SC. The use of all clinical data collected was approved by the local Institutional Review Board for research purposes. The parents gave informed consent for use of the data.

8-Month Pre-operative Model

In order to build a pre-operative model as accurately as possible using the available information, the three-dimensional (3D) geometry of the BDG region was coupled with a lumped parameter model (LPM) of the 8-month-old patient's circulation prior to VVC occlusion. The LPM layout was the same as that presented in Kung *et al.*[11] with the addition of a VVC resistance between the SVC and the single atrium, as well as the APC resistances connecting the aorta to each PA branch. Both clinical data measured at that time and those acquired before undergoing the BDG procedure (in the following called "8-month" and "4-month" clinical data, respectively, for the sake of simplicity) were utilized, as sketched in Fig. 1. The following provides a summary of the developed methodology, which is described in detail in the next sub-Sects.

TABLE 1. Mean pressures and oxygen saturations measured during catheterization.

Location	Mean pressure (mmHg)	O_2 saturation (%)
Superior vena cava	14	41
Inferior vena cava	7	39
Pulmonary arteries	14	45
Left atrium (~pulmonary veins)	7	97
Aorta (~systemic arterial)	66	61
Right atrium	7	41

(1) From the catheterization pressures and O_2 saturations measured prior to VVC closure (i.e., at 8 months), the 8-month mean flow rates and, in turn, the global vascular

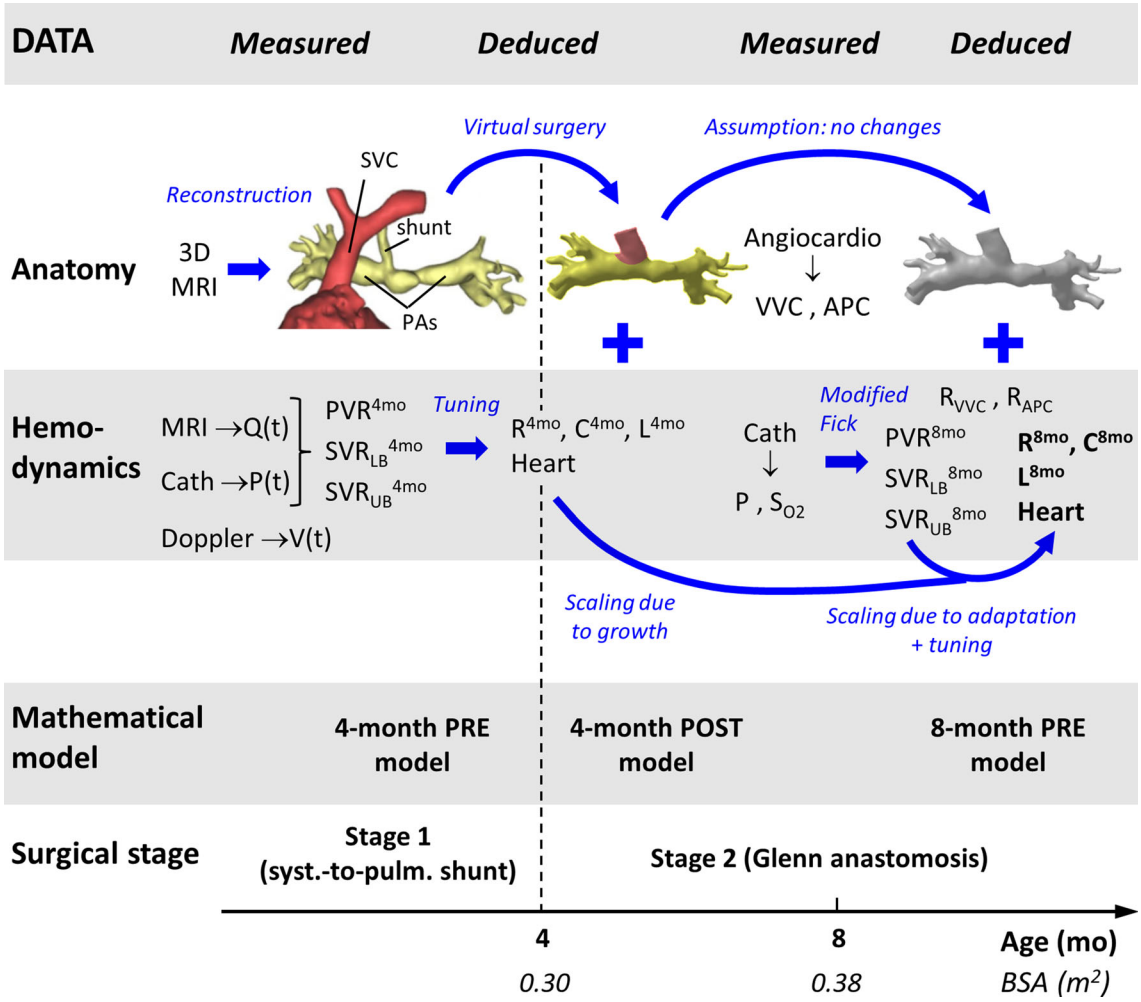

FIGURE 1. Development of the 8-month pre-operative model: 4-month anatomic and hemodynamics data (left) were used to perform the virtual BDG anastomosis and to tune the 4-month cardiovascular lumped parameters (middle left); 8-month angiocardiography revealed the presence of collateral vessels, while catheterization pressures and O_2 saturations allowed to derive the global vascular resistances (middle right); finally the 8-month cardiovascular lumped parameters (right) were obtained by scaling procedures accounting for growth and vascular adaptation.

resistances, as well as the collateral vessels resistances, were derived through the modified Fick method (Fig. 1, *Modified Fick*), accounting for the specific circulatory layout. However, no information (i.e., flow time-tracings) were available to derive the 8-month cardiovascular compliances and inertances.

(2) From the MRI data collected prior to undergo the stage 2 operation (i.e., at 4 months), the PAs and the SVC were reconstructed (Fig. 1, *Reconstruction*) allowing us to perform a virtual BDG surgery (Fig. 1, *Virtual surgery*), whose resulting 3D model was used for our simulations (Fig. 1, *Assumption: no changes*).

(3) The 4-month MRI flows and catheterization pressures (time tracings and mean values) were used to tune the patient-specific lumped parameters of the 4-month circulation (Fig. 1, *Tuning*), following the methodology described in Corsini *et al.*[4]

(4) By applying growth scaling to the 4-month lumped parameters (Fig. 1, *Scaling due to growth*), values of the global vascular resistances were obtained and could be compared with the patient-specific values derived at point 1 in order to evaluate discrepancies. In case of considerable differences, an additional scaling accounting for vascular adaptation (assuming only vasoconstriction or vasodilation) could be applied to the 4-month resistances, and the latter were used to derive the 8-month vascular compliances. Only the heart parameters were tuned to fit the 8-month clinical flow and pressure mean values (Fig. 1, *Scaling due to adaptation + tuning*).

5) The 8-month lumped parameters obtained at point 4 were coupled with the 3D model of point 2, resulting in a closed-loop multi-domain model of the pre-operative circulation, on which a virtual VVC occlusion was performed and the new hemodynamics condition was simulated.

Use of the 8-Month Clinical Data to Derive the 8-Month Vascular Resistances

First, the mean values of pre-operative flow rates through the pulmonary, systemic and collateral circulations were derived from the 8-month measured O_2 saturations. A structural modification to the Fick method (Fig. 1, *Modified Fick*), which is conventionally used by cardiologists to derive flow rates from pressures and O_2 saturations, was necessary due to the combination of BDG circulation with collateral vessels altering arterial and venous O_2 saturations. With reference to Fig. 2, the equations describing the O_2 transport from the lungs to the upper body (UB) and LB were the following:

$$Q_P \cdot (S_{LA} - S_{PA}) \cdot k = V_{O_2} \tag{1}$$

$$Q_{UB} \cdot (S_{art} - S_{SVC}) \cdot k = V_{O_2}^{UB} \tag{2}$$

$$Q_{LB} \cdot (S_{art} - S_{IVC}) \cdot k = V_{O_2}^{LB} \tag{3}$$

Q_P, Q_{UB} and Q_{LB} are the mean values of blood flows (L min^{-1}) through the pulmonary, UB and LB circulations, respectively; S_{LA}, S_{PA}, S_{art}, S_{SVC} and S_{IVC} are the O_2 saturations in the left atrium (i.e., pulmonary veins), pulmonary arteries, aorta, SVC and IVC, respectively. k is the maximal O_2 capacity of blood (mL L^{-1} m^{-2}), calculated as the product of the hemoglobin content (g l^{-1}) and the O_2 binding capacity of hemoglobin (1.34 mL g^{-1}), divided by the patient's BSA. V_{O_2} (mL min^{-1} m^{-2}) represents the total O_2 consumption of systemic tissues and organs, being the sum of the O_2 consumptions in the UB ($V_{O_2}^{UB}$) and in the LB ($V_{O_2}^{LB}$), and equals the O_2 uptake in the lungs.

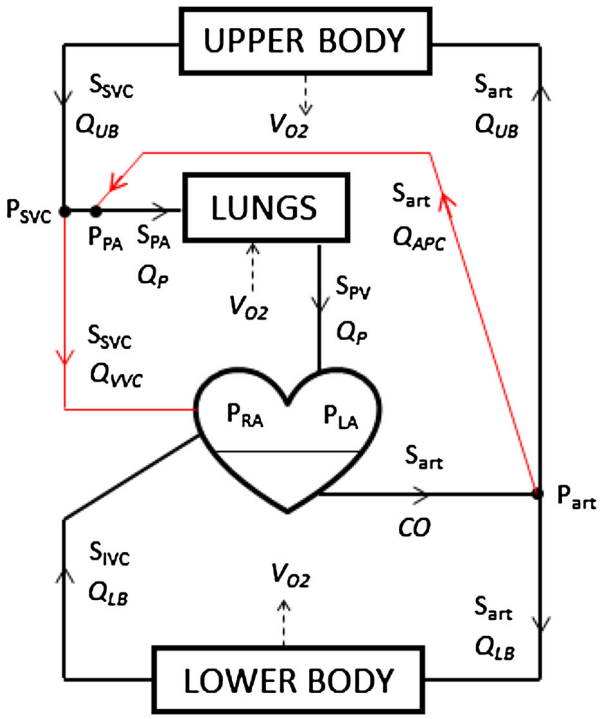

FIGURE 2. Schematic of the patient's circulation with BDG anastomosis and collateral vessels (in red). Pressures, oxygen saturations and flows are indicated with P, S and *Q*, respectively, while *CO* is the cardiac output. The upper body, lungs and lower body blocks denote the respective microcirculations, i.e., where O_2 exchanges (V_{O_2}) take place.

In addition to these, two equations expressing the blood flow balance at the BDG anastomosis, and the O_2 flow balance in the heart, respectively, were formulated as follows:

$$Q_P = Q_{UB} - Q_{VVC} + Q_{APC} \tag{4}$$

$$\begin{aligned} &Q_P \cdot S_{LA} + Q_{VVC} \cdot S_{SVC} + Q_{LB} \cdot S_{IVC} \\ &= (Q_{UB} + Q_{LB} + Q_{APC}) \cdot S_{art} \end{aligned} \tag{5}$$

where Q_{VVC} and Q_{APC} are the VVC and APC flow rate mean values.

It is important to notice that, in this patient's circulation, Q_P was the blood flow crossing the pulmonary microcirculation, hence excluding Q_{VVC} and including Q_{APC}. Moreover, being the sum of Q_{UB} and Q_{LB}, the systemic flow (Q_S) did not equal the cardiac output (CO), as the latter also included Q_{APC}.

In this 5-equation system, the unknowns were six i.e., Q_P, Q_{UB}, Q_{LB}, Q_{VVC}, Q_{APC} and $V_{O_2}^{UB}$ (or $V_{O_2}^{LB}$), with V_{O_2} being usually measured or assumed. Hence, a further assumption was made:

$$V_{O_2}^{UB} = \alpha \cdot V_{O_2} (\text{i.e. } V_{O_2}^{LB} = (1-\alpha) \cdot V_{O_2}) \tag{6}$$

where α is a dimensionless coefficient indicating the V_{O_2} fraction due to the upper body.

As a second step, after deriving Q_P, Q_{UB}, Q_{LB}, Q_{VVC} and Q_{APC} as the solution of the 5-equation system, the 8-month pulmonary, UB and LB systemic vascular resistances (in the following indicated with the superscript "*8mo*"), the VVC and APC resistances were calculated as follows:

$$PVR^{8mo} = \frac{P_{PA} - P_{LA}}{Q_P} \tag{7}$$

$$SVR_{UB}^{8mo} = \frac{P_{art} - P_{SVC}}{Q_{UB}} \tag{8}$$

$$SVR_{LB}^{8mo} = \frac{P_{art} - P_{RA}}{Q_{LB}} \tag{9}$$

$$R_{VVC} = \frac{P_{SVC} - P_{RA}}{Q_{VVC}} \tag{10}$$

$$R_{APC} = \frac{P_{art} - P_{PA}}{Q_{APC}} \tag{11}$$

with P_{PA}, P_{LA}, P_{art}, P_{SVC} and P_{RA} being the mean pulmonary artery, left atrium, aortic, SVC and right atrium pressures, respectively.

From the simple representation of the patient's circulation in Fig. 2, it is however possible to notice that the BDG region is characterized by a complicated network of non-physiological connections between several vessels including the collateral ones. Therefore, for the present study the multi-domain approach was preferred, rather than a pure lumped parameters approach, to directly account for the local energy dissipations that might be caused by the 3D geometry.

Use of the 4-Month Clinical Data to Build the 8-Month Pre-operative Model

Although the PVR^{8mo}, SVR_{UB}^{8mo} and SVR_{LB}^{8mo} were estimated, the individual compliances, inertances and heart parameters could not be inferred from the 8-month clinical data available (i.e., no time tracings, but only mean values). Furthermore, the 3D geometry of the BDG region that had to be coupled with the LPM, in order to complete the multi-domain model of the 8-month-old patient's circulation, was unknown. Hence, for all of them, the clinical information acquired at 4 months (i.e., before the patient underwent the BDG procedure) was exploited as described below.

First, a multi-domain model of the 4-month-old patient's circulation was developed, following the methodological approach described in Corsini *et al.*[4] A 3D model of the patient's shunt, its PA anastomosis and the first PA branches, including the stenosis, was reconstructed from MRI data which were acquired prior to the BDG procedure (Fig. 1, *Reconstruction*). Based on the pre-operative flow and pressure data collected and this 3D model, the global resistances (PVR^{4mo}) and the local lumped parameters representing the pulmonary vasculature were calibrated. Then, the global systemic resistances (SVR_{UB}^{4mo} and SVR_{LB}^{4mo}) and the individual compliances, inertances and heart parameters were set up (Fig. 1, *Tuning*). After the patient underwent BDG surgery, no imaging data were acquired. However, by reconstructing the patient's 3D SVC from the pre-stage 2 data (Fig. 1, *Reconstruction*), a virtual BDG anastomosis was performed, namely the shunt was removed and the SVC was connected to the main RPA, also removing the left PA stenosis (Fig. 1, *Virtual surgery*). The final geometry resulting from the virtual procedure was supervised and approved by the physicians and surgeons who followed the clinical case. The multi-domain model, coupling the 3D virtual BDG geometry with the pre-BDG LPM, is partially described in Kung *et al.*[11] except for the virtual surgery performed, i.e., BDG anastomosis instead of hemi-Fontan connection.

Then, the PVR^{4mo}, SVR_{UB}^{4mo} and SVR_{LB}^{4mo} were compared with the PVR^{8mo}, SVR_{UB}^{8mo} and SVR_{LB}^{8mo}. In general, since local vascular resistances (R) are related to local vascular length (l) and diameter (d) as follows:

$$R \propto \frac{l}{d^4} \tag{12}$$

and l and d are proportional to the square root of the BSA, decreases in all resistances were expected due to growth, that means increases in both l and d passing from BSA^{4mo} to BSA^{8mo}. Similarly, since local compliances (C) and inertances (L) are related to l and d as:

$$C \propto l \cdot d^3 \text{ and } L \propto \frac{l}{d^2} \tag{13}$$

C and L were expected to increase and decrease, respectively, with the BSA.

Using allometric equations, proper scaling factors were applied to the 4-month local R, C and L (Fig. 1, *Scaling due to growth*) to account for the BSA increase[19] and for the different vessel growths in the lungs, UB and LB.[2,3] The resulting $PVR^{8mo,g}$, $SVR_{UB}^{8mo,g}$ and $SVR_{LB}^{8mo,g}$ (with "g" denoting growth) were compared with the patient-specific PVR^{8mo}, SVR_{UB}^{8mo} and SVR_{LB}^{8mo} to evaluate discrepancies. In fact, any differences between the three couples of vascular resistances would suggest that phenomena other than growth did occur during the four months elapsed from BDG surgery, and, therefore, would require consideration in the pre-operative LPM development. In particular, given the relationships 12 and 13, and assuming that such phenomena involved only diameter changes (i.e., vasoconstrictions or vasodilatations), the patient-specific vascular compliances (C^{8mo}) could be derived from those which only account for growth ($C^{8mo,g}$), and from the corresponding resistances (R^{8mo} and $R^{8mo,g}$, with $R = PVR$, SVR_{UB} or SVR_{LB}), using the following expression[1]:

$$C^{8mo} = C^{8mo,g} \cdot \left(\frac{R^{8mo}}{R^{8mo,g}}\right)^{-\frac{3}{4}} \tag{14}$$

As the last step to complete the patient-specific LPM, the 4-month heart parameters were tuned to obtain the 8-month flows and pressures (Fig. 1, *Scaling due to adaptation + tuning*).[4] Finally, the 3D virtual BDG geometry was coupled with the 8-month LPM (Fig. 3) and a pulsatile simulation was run, verifying the results matching with the patient-specific clinical data. The heart rate was set as 107 beats per minute, being the value measured during the cardiac catheterization exam. As the boundary conditions for the 3D domain, the pressures calculated at the 3D boundaries, by solving the LPM equations at each time step, were uniformly applied to the corresponding inlet or outlet cross-sections.[17] It is worthwhile noting that BDG anatomy was assumed as unchanged after stage 2 surgery, since no accurate imaging data could be used to reconstruct the 8-month BDG geometry (Fig. 1, *Assumption*).

The 3D rigid-walled domain was meshed with an unstructured tetrahedral grid of 1.2 million elements, based on grid sensitivity analyses performed in

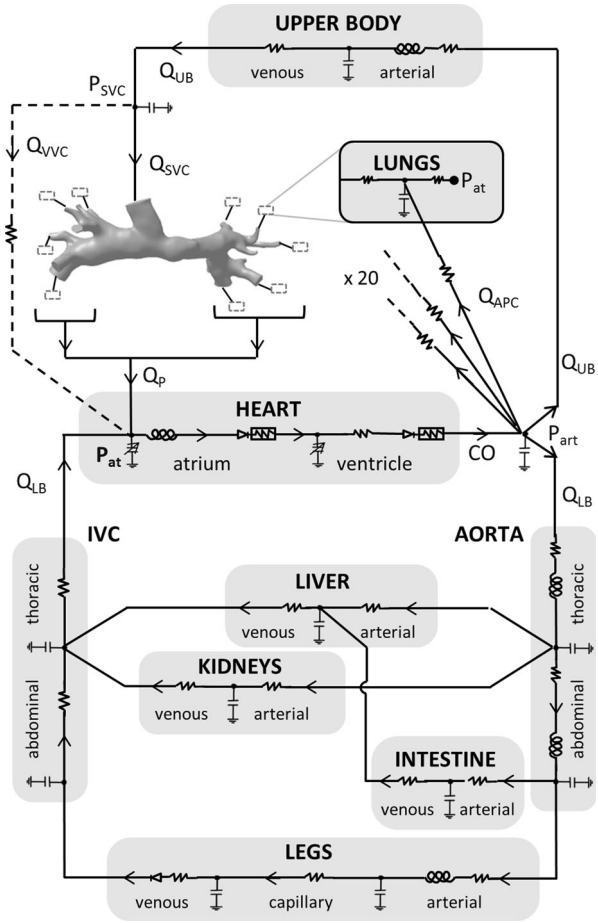

FIGURE 3. 8-month multi-domain model with collateral vessels. The 3D model of the BDG anastomosis is coupled with the vascular and heart lumped parameters, including the veno-venous collateral vessel (dashed line) which will be removed to perform virtual occlusion, and the aorto-pulmonary collateral vessels connected to each pulmonary artery branch (i.e., 20).

previous studies from our group.[2,18] This mesh size was in agreement with those used in other studies simulating similar anatomies.[4,11,21] Using commercial software ANSYS ICEM CFD 14.0 (ANSYS Inc., Canonsburg, PA, USA), the maximum element size was set as 0.7 10^{-3} m, and automatic mesh refinement in proximity of curves was enabled. The simulation was run using the finite volume code ANSYS Fluent, with 2nd order spatial discretization for momentum and pressure, and the 1st order implicit transient formulation to solve the Navier–Stokes equations in the 3D domain. Blood was assumed as a Newtonian fluid with density of 1060 kg m^{-3} and dynamic viscosity of 0.004 Pa s. The explicit Euler time-marching scheme was used to solve the LPM equations system, with a time step of 10^{-4} s for six cardiac cycles to guarantee the solution periodicity. The time step Δt was derived based on the Courant–Friedrichs–Lewy condition limiting the Courant number ($C = \frac{u\Delta t}{x}$, with u being the mean flow velocity

within the 3D domain, and Δx the average edge size of grid cells) to be lower than 1. Note that the Δt obtained by applying this condition guarantees stability of the Navier–Stokes solution, and works efficiently also for the explicit Euler method solution.[20]

Results from the last cardiac cycle were used in the analysis (i.e., mean values calculation). Simulations were run using a parallel cluster compute node, with two Quad-Core Intel Xeon E5620 processors, requiring about 1.5 h per cardiac cycle.

8-Month Post-operative Model

The VVC closure was performed by simply removing the VVC resistance from the LPM (Fig. 3, dashed line), and accordingly modifying the LPM equation system. Another pulsatile simulation was performed with the same settings as described above. Post-operative O_2 saturations were calculated using the flow rates resulting from the simulation, and the Eqs. (1)–(6), assuming S_{LA}, V_{O_2} and α unchanged from the pre-operative scenario. To this end, one should bear in mind that the atrium model consisted of a single block representing the left and right chambers communicating through a non-obstructive septal defect. Hence, for the models results and calculations, it was not possible to distinguish between left and right atria.

RESULTS

Assuming in Eqs. (1)–(11) $\alpha = 0.5$ and $V_{O_2} = 170$ mL min^{-1} m^{-2}, as a reasonable value derived from the patient's anthropometric data and weight-based relationships,[12] the mean flow rates and vascular resistances reported in Table 2 were derived. It is worthwhile noting that Q_p did not equal Q_{UB} because of the presence of collateral vessels originating from the UB veins. CO was equal to 1.57 L min^{-1}, with $Q_S = 1.45$ L min^{-1} and a pulmonary to systemic flow ratio of 0.4. Q_{VVC} resulted to be 18.5% CO, i.e., about 2.4 times Q_{APC}.

TABLE 2. Patient-specific 8-month flow rates and vascular resistances.

Location	Mean flow (L min^{-1})	Vascular resistance (WU)
Upper body	0.76	69.1
Lower body	0.69	86.2
Pulmonary	0.59	12.1
Veno-venous collateral	0.29	24.2
Aorto-pulmonary collateral	0.12	449.0

WU = mmHg min l^{-1}.

Figure 4 outlines the changes in global vascular resistances occurred in the four months elapsed from the BDG surgery to the VVC treatment. Considering the changes due to growth (i.e., from $BSA^{4mo} = 0.3$ m^2 to $BSA^{8mo} = 0.38$ m^2), the PVR, SVR_{UB} and SVR_{LB} should have decreased by about 22, 13 and 25%, respectively, reaching the following values: $PVR^{8mo,g} = 8.08$ WU, $SVR_{UB}^{8mo,g} = 122$ WU and $SVR_{LB}^{8mo,g} = 103$ WU (WU = mmHg min L^{-1}). These values did not correspond to the patient-specific values obtained above (Table 2), namely $PVR^{8mo} = 12.1$ WU, $SVR_{UB}^{8mo} = 69.1$ WU and $SVR_{LB}^{8mo} = 86.2$ WU, which instead indicated 17% increase in PVR, 51% decrease in SVR_{UB} and 37% decrease in SVR_{LB}.

The C^{8mo} of the LPM were obtained by applying Eq. (14). The heart model parameters were tuned accordingly, thus completing the 8-month pre-operative LPM to couple with the 3D BDG geometry. A multi-domain simulation was carried out, resulting in flows and pressures matching the patient-specific values (Table 1 for pressures and Table 2 for flows) with differences lower than 5%.

Table 3 reports the mean pressures and flows obtained by simulating the post-operative scenario, i.e., by removing the VVC resistance, and the post-operative O_2 saturations calculated using the Eqs. (1)–(6). Considering BDG pressure as the average of the pressures recorded at the inlet (P_{SVC}) and the outlets (P_{PA}) of the 3D model, the multi-domain results showed an increase by 2 mmHg with respect to the pre-operative scenario (from 14 to 16 mmHg). CO decreased by 7.0% (1.46 vs. 1.57 L min^{-1}). However,

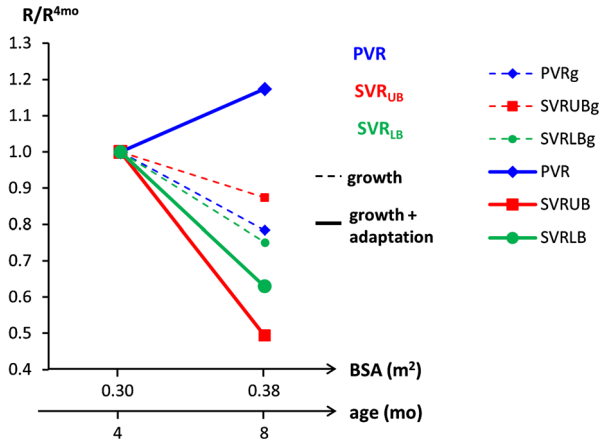

FIGURE 4. Changes in global vascular resistances from BDG surgery (BSA = 0.30 m^2) to VVC occlusion (BSA = 0.38 m^2). Resistance values are normalized over the 4-month corresponding values (PVR^{4mo} = 10.3 WU, SVR_{UB}^{4mo} = 140 WU, SVR_{LB}^{4mo} = 137 WU). Predicted changes due to growth are shown with dashed lines, while clinically observed changes (i.e. due to growth and adaptation) are depicted with solid lines.

the post-operative O_2 saturations improved, in particular S_{art} increased from 61 to 78%, S_{SVC} from 41 to 56%, and S_{IVC} from 39 to 55%. It is worth noting that, after VVC removal, PA flow equaled Q_{UB} (indicated as SVC flow in Table 3).

Figure 5 depicts the wall pressure maps and velocity vectors of the 3D domain before and after VVC closure. Overall, the models exhibited typical pressure and velocity distributions, as in Troianowski *et al.*[21] Wall pressure distributions resulted comparable pre- and post-operatively, although with differences of approximately 2 mmHg. Similarly, velocity vectors showed flow impingement on the inferior wall at the anastomotic level in both geometries, as well as comparable flow splitting between left and right, but the post-operative model presented higher velocity magnitudes due to the increased inlet flow rate.

TABLE 3. Predicted results after virtual VVC occlusion.

Location	Mean pressure (mmHg)	Mean flow (L min^{-1})	O_2 saturation (%)
Superior vena cava	17	0.68	56
Inferior vena cava	6.4	0.67	55
Pulmonary arteries	15	0.68	59
Aorta (~systemic arterial)	64	1.46	78
Left/right atrium	6.2	N.A.	N.A.

DISCUSSION

Patients with single ventricle defects are usually palliated with a multi-staged procedure which gradually by-passes the non-functioning ventricle, while allowing the vascular bed to grow, and the hemodynamics to stabilize before undergoing the next surgical stage. However, during the inter-stage periods, those patients are prone to develop further cardiovascular complications, e.g., collateral vessel formation or heart valve dysfunction. Clinical studies reported the presence of systemic venous collateral vessels in about 31–33% of patients who underwent a BDG procedure, and associated this occurrence to several alterations of the physiological hemodynamics.[14,16] For example, by performing a BDG anastomosis the lungs will be perfused by the UB flow, which is considerably higher compared to the shunt flow. In this scenario, the pulmonary circulation might start suffering from hypertension (i.e., 13 ± 4 mmHg vs. 11 ± 4 mmHg), and the UB would not drain properly due to the consequent SVC pressure increase (i.e., 14 ± 5 mmHg vs.

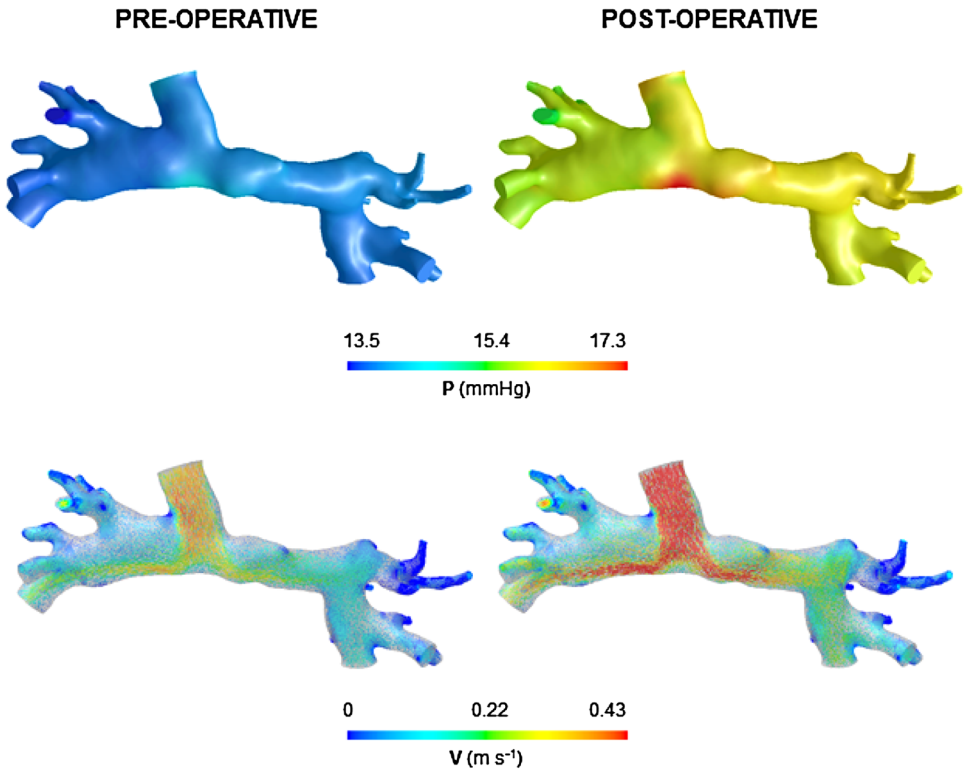

FIGURE 5. Wall pressure maps (top) and velocity vectors (bottom) of the pre-operative (left) and post-operative (right) models at peak inlet flow.

11 ± 4 mmHg). At the same time, the atrial pressure might decrease (i.e., 5 ± 2 mmHg vs. 6 ± 3 mmHg) owing to the atrial inflow reduction, hence a possible outcome would be the formation of decompressing collateral vessels in the interested region.[14]

In this study, a multi-domain model of an 8-month-old BDG patient affected by multiple collateral vessels (VVC and APC) was developed, and a virtual surgery occluding the major VVC was performed. Closure of VVC is often performed in single ventricle patients with stage 2 physiology in order to improve O_2 saturation. While an elevation in the BDG pressure is an expected finding, the degree of elevation can be hard to otherwise predict and is clinically relevant. Furthermore, while it is assumed that occlusion of a VVC will result in an increase in O_2 saturation, this change is not always present in real life. Alteration in the systemic blood flow can result in a decrease in mixed venous saturation. This can attenuate, or even overcome, the expected change in O_2 saturation. Also, while the systemic O_2 saturation may increase with occlusion, a significant decline in systemic blood flow may decrease the overall systemic O_2 delivery. Patient specific modeling, as described in this manuscript, carries the potential of providing this quantitative information before a procedure is performed, so that clinicians can make a more informed decision about the expected outcomes of the procedure.

The closed-loop multi-domain approach enabled us (i) to directly account for the local energy dissipations due to the complex hemodynamics of the 3D anastomotic region which was involved in collateral vessel formation, and (ii) to directly incorporate changes in vascular impedances occurring after VVC closure. The principal aim of this work was to show how it is possible to build a reliable pre-operative model by integrating all the clinical data available, including those acquired at the time of BDG surgery. Furthermore, the model could be used to predict the hemodynamics after collateral vessel closure, showing, as expected, an increase in the O_2 saturations whereas a decrease in CO. Moreover, it confirmed the BDG pressure rise which was clinically observed. Although it may seem small, a 2 mmHg PA pressure increase in patients with single ventricle physiology may not be negligible, insomuch that a decompressing drug therapy might be necessary, as was the case of the investigated patient.

From the catheterization pressures and O_2 saturations acquired just before VVC closure, it was possible to estimate the flow rates and, thus, the vascular resistances using a ''corrected'' Fick method, i.e., suitable for a BDG circulation with VVC and APC. In the absence of flow and pressure time tracings to derive and tune the whole vascular impedances (i.e., compliances and inertances), the 4-month post-operative BDG model, which was previously developed based on the pre-BDG patient-specific data,[4,11] was utilized. A scaling methodology accounting for the physical growth of the patient was applied to the 4-month BDG model, allowing us to detect differences between the resistances evaluated from the 8-month catheterization data set, and those resulting from the scaling procedure (Fig. 4). This suggested that vascular adaptation mechanisms occurred during the four months elapsed between the BDG procedure and VVC occlusion, namely PVR vasoconstriction (12.1 WU vs. 8.08 WU) whereas SVR_{UB} and SVR_{LB} vasodilatations (69.1 WU vs. 122 WU and 86.2 WU vs. 103 WU, respectively). A recent work showed that local high and low shear stresses, associated with abnormal pulmonary flow, may alter the pulmonary vascular tone, increasing the PVR.[13] Therefore, the non-physiological pulmonary flow due to the BDG surgery in the investigated patient might have caused mid-term adaptations in the pulmonary vasculature, thus explaining the apparent PVR vasoconstriction. The findings of the present study highlighted the importance of taking into account the adaptive phenomena that might happen in complex hemodynamics such as univentricular circulations, when developing a patient-specific model from a previous mathematical representation of the younger patient. Scientific effort has been made to reproduce, using mathematical modeling, adaptive phenomena such as the short-term responses of the coronary circulation to physiological changes following exercise,[10] or cerebro-vascular regulation mechanisms in response to external and pathological perturbations.[7] Nevertheless, to the best of our knowledge, mid/long-term adaptive phenomena have not been considered in patient-specific models for pre-operative planning.

Another important issue is the amount of data collected for building up a customized model. In order to reduce the procedural risk for the patient, it is common practice for physicians to acquire only the data necessary to a have a clinically acceptable overview of the patient scenario, prior to performing the surgical treatment. With regard to the present clinical case, the lack of an extensive data set led to assumptions about V_{O_2} and the partial consumptions due the UB and the LB, to calculate blood flows. These hypotheses were based on mathematical relationships expressing the V_{O_2} increase with body weight, and on the reasonable assumption that, in an 8-month-old baby, the development of the UB vasculature is comparable to that of the LB vasculature. For example, considering 12% uncertainty related to V_{O_2} assumption (i.e., V_{O_2} ranging from 150 to 190 mL min^{-1} m^{-2}) in accordance with V_{O_2} values estimated using height-based or BSA-based relationships,[12] the estimated flow rates and vascular resistances varied by 9.3 and 9.4%,

respectively, from the values reported in Table 2. The uncertainties resulting for SVR_{UB}^{8mo} (i.e., ranging from 62.6 to 75.6 WU) still indicated a considerable decrease with respect to $SVR_{UB}^{8mo,g}$ (122 WU), as highlighted above. On the contrary, the uncertainties resulting for PVR^{8mo} (i.e., ranging from 11 to 13 WU) showed significant increase compared with $PVR^{8mo,g}$ (8.1 WU) and even with PVR^{4mo} (10 WU). The SVR_{LB}^{8mo} values considering the uncertainties (i.e., ranging from 78.1 to 94.3 WU) were lower than $SVR_{LB}^{8mo,g}$ (103 WU), but with less significance. These findings fairly suggested that vasoconstriction occurred in the pulmonary vasculature, while vasodilatation in the UB, being in accordance with SVC and PA hypertension potentially leading to VVC formation.[14] Based on the clinical findings about VVC formation after the BDG surgery,[14,16] a virtual post-stage 2 model could also indicate whether the patient is prone to develop VVCs, depending on the predicted P_{SVC}, P_{PA} and trans-pulmonary pressure gradient.

Additional uncertainty factors were associated to pressure and flow measurements prior to BDG surgery. As usually happens with stage 1 patients, the presence of the tight shunt hindered a direct access to the pulmonary arteries for catheter pressure acquisition. Hence, P_{PA} was evaluated by means of the pulmonary venous wedge pressure (PVWP). Although PVWP overall provides an accurate estimate of P_{PA},[9] 1 to 3 mmHg uncertainty remains. Moreover, the high velocity and often turbulent flow characterizing the shunt region may cause MRI signal loss, leading to about 10% uncertainty in Q_P measurement. If, for instance, the 4-month P_{PA} (12 mmHg) is varied by only ± 1 mmHg, and the 4-month Q_P (0.58 L min^{-1}) is varied by $\pm 10\%$, the PVR^{4mo} would range from 7.8 WU to 13 WU. The upper limit (13 WU) suggested that the mild vasoconstriction apparently occurred in the lungs (see the above explanation) might be negligible, since the PVR^{8mo} values obtained accounting for V_{O_2} uncertainty would be ascribable only to the patient's growth.

These considerations about clinical data uncertainties underlined the importance of (i) collecting a full data set with simultaneous acquisitions of pressures and flows, when possible, and (ii) taking into account the vascular adaptive mechanisms potentially occurring after a BDG procedure, for developing an accurate patient-specific model while limiting the number of assumptions. The approach presented in this study was limited by the impossibility to compare the modeling results with an extensive clinical dataset post-operatively collected, and by the absence of a cohort of patients for whom the methodology could be verified. However, such study could motivate the post-operative collection of data such as O_2 saturations and systemic blood flow which are important clinical outcomes. Although only one clinical case was considered in the present work, the developed approach can be similarly applied to other patients in the same situation or requiring additional treatment (not necessarily collateral vessel closure) after the main surgery, in case heterogeneous, patient-specific clinical data were collected at different times. Certain improvement in clinical data acquisition, thus in the set-up of the model vascular resistances, can be reached by measuring the patient-specific V_{O_2}. This data could be available in ordinary clinical practice as it is a non-invasive and low-cost measurement. On the contrary, to introduce patient-specific modeling for growth and adaptation, based on clinical data, is not feasible. Anyhow, the impact of the assumptions made in the allometric equations is high only for large distances between the two data collection times. In the present case, only four months elapsed from the BDG operation and the VVC closure, therefore the uncertainty effect on vascular parameter estimation is reduced.

Our methodology represents a further step towards personalized medicine, where the close collaboration between modelers and clinicians, along with the advancements in computer science and biomedical technologies, might reduce the gaps and help the clinical decision making. To this end, it is essential that the modeling approach is able to face and overcome the constraints of the clinical practice with small babies affected by multiple and complex CHD, i.e., the considerable difficulty with routinely collecting a full dataset.

ACKNOWLEDGMENTS

This study was supported by Fondation Leducq, Paris, through the Trans-Atlantic Network of Excellence for Cardiovascular Research grant 'Multi-Scale Modelling of Single Ventricle Hearts for Clinical Decision Support'.

CONFLICT OF INTEREST

None.

REFERENCES

[1]Baretta, A., C. Corsini, A. L. Marsden, I. E. Vignon-Clementel, T.-Y. Hsia, G. Dubini, F. Migliavacca, and G. Pennati, The Modeling of Congenital Hearts Alliance (MOCHA). Respiratory effects on hemodynamics in

patient-specific CFD models of the Fontan circulation under exercise conditions. *Eur. J. Mech. B-Fluid.* 35:61–69, 2012.

[2]Baretta, A., C. Corsini, W. Yang, I. E. Vignon-Clementel, A. L. Marsden, J. A. Feinstein, T.-Y. Hsia, G. Dubini, F. Migliavacca, G. Pennati, and The Modeling of Congenital Hearts Alliance (MOCHA) Investigators. Virtual surgeries in patients with congenital heart disease: a multi-scale modelling test case. *Philos. Trans. R. Soc. A* 369:4316–4330, 2011.

[3]Coppoletta, J. M., and S. B. Wolbach. Body length and organ weights of infants and children. A study of the body length and normal weights of the more important vital organs of the body between birth and twelve years of age. *Am. J. Pathol.* 9:55–70, 1933.

[4]Corsini, C., C. Baker, E. Kung, S. Schievano, G. Arbia, A. Baretta, G. Biglino, F. Migliavacca, G. Dubini, G. Pennati, A. Marsden, I. Vignon-Clementel, A. Taylor, T. Y. Hsia, and A. Dorfman for the Modeling of Congenital Hearts Alliance Mocha Investigators. An integrated approach to patient-specific predictive modeling for single ventricle heart palliation. *Comput. Methods Biomech. Biomed. Eng.* 17:1572–1589, 2014.

[5]de Zélicourt, D. A., C. M. Haggerty, K. S. Sundareswaran, B. S. Whited, J. R. Rossignac, K. R. Kanter, J. W. Gaynor, T. L. Spray, F. Sotiropoulos, M. A. Fogel, and A. P. Yoganathan. Individualized computer-based surgical planning to address pulmonary arteriovenous malformations in patients with a single ventricle with an interrupted inferior vena cava and azygous continuation. *J. Thorac. Cardiovasc. Surg.* 141:1170–1177, 2011.

[6]Fontan, F., and E. Baudet. Surgical repair of tricuspid atresia. *Thorax* 26:240–248, 1971.

[7]Giannessi, M., M. Ursino, and W. B. Murray. The design of a digital cerebrovascular simulation model for teaching and research. *Anesth. Analg.* 107:1997–2008, 2008.

[8]Haggerty, C. M., D. A. de Zelicourt, K. Sundareswaran, K. Pekkan, B. Whited, J. Rossignac, M. A. Fogel, and A. P. Yoganathan. Hemodynamic assessment of virtual surgery options for a failing Fontan using lumped parameter simulation. *Comput. Cardiol.* 36:389–392, 2009.

[9]Hill, K. D., D. Janssen, D. P. Ohmstede, and T. P. Doyle. Pulmonary venous wedge pressure provides a safe and accurate estimate of pulmonary arterial pressure in children with shunt-dependent pulmonary blood flow. *Catheter. Cardiovasc. Interv.* 74:747–752, 2009.

[10]Kim, H. J., K. E. Jansen, and C. A. Taylor. Incorporating autoregulatory mechanisms of the cardiovascular system in three-dimensional finite element models of arterial blood flow. *Ann. Biomed. Eng.* 38:2314–2330, 2010.

[11]Kung, E., A. Baretta, C. Baker, G. Arbia, G. Biglino, C. Corsini, S. Schievano, I. E. Vignon-Clementel, G. Dubini, G. Pennati, A. Taylor, A. Dorfman, A. M. Hlavacek, A. L. Marsden, T. Y. Hsia, F. Migliavacca, and the Modeling of Congenital Hearts Alliance (MOCHA) Investigators. Predictive modeling of the virtual Hemi-Fontan operation for second stage single ventricle palliation: two patient-specific cases. *J. Biomech.* 46:423–429, 2013.

[12]Li, J., A. Bush, I. Schulze-Neick, D. J. Penny, A. N. Redington, and L. S. Shekerdemian. Measured versus estimated oxygen consumption in ventilated patients with congenital heart disease: the validity of predictive equations. *Crit. Care Med.* 31:1235–1240, 2003.

[13]Li, M., D. E. Scott, R. Shandas, K. R. Stenmark, and W. Tan. High pulsatility flow induces adhesion molecule and cytokine mRNA expression in distal pulmonary artery endothelial cells. *Ann. Biomed. Eng.* 37:1082–1092, 2009.

[14]Magee, A. G., B. W. McCrindle, J. Mawson, L. N. Benson, W. G. Williams, and R. M. Freedom. Systemic venous collateral development after the bidirectional cavopulmonary anastomosis. Prevalence and predictors. *J. Am. Coll. Cardiol.* 32:502–508, 1998.

[15]Marsden, A. L. Simulation based planning of surgical interventions in pediatric cardiology. *Phys. Fluids* 25:101303, 2013.

[16]McElhinney, D. B., V. M. Reddy, F. L. Hanley, and P. Moore. Systemic venous collateral channels causing desaturation after bidirectional cavopulmonary anastomosis: evaluation and management. *J. Am. Coll. Cardiol.* 30:817–824, 1997.

[17]Migliavacca, F., R. Balossino, G. Pennati, G. Dubini, T. Y. Hsia, M. R. de Leval, and E. L. Bove. Multiscale modelling in biofluidynamics: application to reconstructive paediatric cardiac surgery. *J. Biomech.* 39:1010–1020, 2006.

[18]Pennati, G., C. Corsini, D. Cosentino, T. Y. Hsia, V. S. Luisi, G. Dubini, and F. Migliavacca. Boundary conditions of patient-specific fluid dynamics modelling of cavopulmonary connections: possible adaptation of pulmonary resistances results in a critical issue for a virtual surgical planning. *Interface Focus* 1:297–307, 2011.

[19]Pennati, G., and R. Fumero. Scaling approach to study the changes through the gestation of human fetal cardiac and circulatory behaviors. *Ann. Biomed. Eng.* 28:442–452, 2000.

[20]Quarteroni, A., S. Ragni, and A. Veneziani. Coupling between lumped and distributed models for blood flow problems. *Comput. Visual. Sci.* 4:111–124, 2001.

[21]Troianowski, G., C. A. Taylor, J. A. Feinstein, and I. E. Vignon-Clementel. Three-dimensional simulations in BDG patients: clinically based boundary conditions, hemodynamic results and sensitivity to input data. *J. Biomech. Eng.* 133:111006, 2011.

[22]Vignon-Clementel, I. E., A. L. Marsden, and J. A. Feinstein. A primer on computational simulation in congenital heart disease for the clinician. *Prog. Pediatr. Cardiol.* 30:3–13, 2010.